A peer-reviewed version of this preprint was published in PeerJ on 14 March 2017.

View the peer-reviewed version (peerj.com/articles/3087), which is the preferred citable publication unless you specifically need to cite this preprint.

Tejral G, Sopko B, Necas A, Schoner W, Amler E. (2017) Computer modelling reveals new conformers of the ATP binding loop of Na^+/K^+-ATPase involved in the transphosphorylation process of the sodium pump. PeerJ 5:e3087 https://doi.org/10.7717/peerj.3087

Computer modelling reveals new conformers of the ATP binding loop of Na^+/K^+-ATPase involved in the transphosphorylation process of the sodium pump

Gracian Tejral [1, 2], **Bruno Sopko** [3], **Alois Necas** [4], **Wilhelm Schoner** [5], **Evzen Amler** Corresp. [1, 2]

[1] Department of Biophysics, 2nd Faculty of Medicine, Charles University Prague, Prague, Czech Republic

[2] Laboratory of Tissue Engineering, Institute of Experimental Medicine, Academy of Sciences of the Czech Republic, Prague, Czech Republic

[3] Department of Medical Chemistry and Clinical Biochemistry, 2nd Faculty of Medicine, Charles University Prague, Prague, Czech Republic

[4] Small Animal Clinic, Faculty of Veterinary Medicine, University of Veterinary and Pharmaceutical Science, Brno, Czech Republic

[5] Institute of Biochemistry and Endocrinology, University of Giessen, Giessen, Germany

Corresponding Author: Evzen Amler
Email address: evzen.amler@lfmotol.cuni.cz

Hydrolysis of ATP by Na^+/K^+-ATPase, a P-Type ATPase, catalyzing active Na^+ and K^+ transport through cellular membranes leads transiently to a phosphorylation of its catalytical α-subunit. Surprisingly, 3-dimensional molecular structure analysis of P-type ATPases reveals that binding of ATP to the N-domain connected by a hinge to the P-domain is much too far away from the Asp^{369} to allow the transfer of ATP's terminal phosphate to its aspartyl-phosphorylation site. In order to get information how the transfer of the γ-phosphate group of ATP to the Asp^{369} is achieved, analogous molecular modeling of the M_4-M_5 loop of ATPase was performed using the crystal data of Na^+/K^+-ATPase of different species. Analogous molecular modeling of the cytoplasmic loop between Thr^{338} and Ile^{760} of the α_2-subunit of Na^+/K^+-ATPase and the analysis of distances between the ATP binding site and phosphorylation site revealed the existence of 2 ATP binding sites in the open conformation, the first one close to Phe^{475} in the N-domain, the other one close to Asp^{369} in the P-domain. However, binding of Mg^{2+}•ATP to any of these sites in the "open conformation" may not lead to phosphorylation of Asp^{369}. Additional conformations of the cytoplasmic loop were found wobbling between "open conformation" <==> "semi-open conformation <==> "closed conformation" in the absence of $2Mg^{2+}$•ATP. The cytoplasmic loop's conformational change to the "semi-open conformation" -- characterized by a hydrogen bond between Arg^{543} and Asp^{611} -- triggers by binding of $2Mg^{2+}$•ATP to a single ATP site and conversion to the "closed conformation" the phosphorylation of Asp^{369} in the P-domain, and hence the start of Na^+/K^+-activated ATP hydrolysis.

Computer modelling reveals new conformers of the ATP binding loop of Na^+/K^+-ATPase involved in the transphosphorylation process of the sodium pump

G. Tejral[1,2], B. Sopko[3], A. Necas[4], W. Schoner[5] and E. Amler[1,2]

[1]Laboratory of Tissue Engineering, Institute of Experimental Medicine, Academy of Sciences of the Czech Republic, Prague, Czech Republic,

[2]Department of Biophysics, 2nd Faculty of Medicine, Charles University, Prague, Czech Republic,

[3]Department of Medical Chemistry and Clinical Biochemistry, 2nd Faculty of Medicine, Charles University and Motol University Hospital, Prague, Czech Republic,

[4]Small Animal Clinic, Faculty of Veterinary Medicine, University of Veterinary and Pharmaceutical Sciences Brno, Brno, Czech Republic

[5]Institute of Biochemistry and Endocrinology, University of Giessen, Giessen, Germany

Corresponding author: Evžen Amler, Prof., PhD., Charles University in Prague, 2nd Faculty of Medicine, Department of Biophysics, V Úvalu 84, 150 06 Prague 5, Czech Republic. Phone: +420 257 296 350, Fax: +420 257 296 355, E-mail: evzen.amler@lfmotol.cuni.cz

Abstract

Hydrolysis of ATP by Na^+/K^+-ATPase, a P-Type ATPase, catalyzing active Na^+ and K^+ transport through cellular membranes leads transiently to a phosphorylation of its catalytical α-subunit. Surprisingly, 3-dimensional molecular structure analysis of P-type ATPases reveals that binding of ATP to the N-domain connected by a hinge to the P-domain is too far away from the Asp^{369} to allow the transfer of ATP's terminal phosphate to its aspartyl-phosphorylation site. In order to

get information on how the transfer of the γ-phosphate group of ATP to the Asp^{369} is achieved, analogous molecular modeling of the M_4-M_5 loop of ATPase was performed using the crystal data of Na^+/K^+-ATPase of different species. Analogous molecular modeling of the cytoplasmic loop between Thr^{338} and Ile^{760} of the α_2-subunit of Na^+/K^+-ATPase and the analysis of distances between the ATP binding site and phosphorylation site revealed the existence of 2 ATP binding sites in the open conformation, the first one close to Phe^{475} in the N-domain, the other one close to Asp^{369} in the P-domain. However, binding of Mg^{2+}•ATP to any of these sites in the "open conformation" may not lead to phosphorylation of Asp^{369}. Additional conformations of the cytoplasmic loop were found wobbling between "open conformation" <==> "semi-open conformation <==> "closed conformation" in the absence of $2Mg^{2+}$•ATP. The cytoplasmic loop's conformational change to the "semi-open conformation" (characterized by a hydrogen bond between Arg^{543} and Asp^{611}) triggers by binding of $2Mg^{2+}$•ATP to a single ATP site and conversion to the "closed conformation" the phosphorylation of Asp^{369} in the P-domain, and hence the start of Na^+/K^+-activated ATP hydrolysis.

Introduction

Na^+/K^+-ATPase (EC 3.6.3.9) is an integral membrane protein that transports sodium and potassium ions against an electrochemical gradient. It belongs to the family of P-type ATPases that is structurally typified by the L-2-haloacid dehalogenase. Na^+/K^+-ATPase and Ca^{2+}-ATPase belong to this family and show a high degree of homology, especially at the phosphorylation domain. The tertiary structure of Na^+/K^+-ATPase has been solved at high resolution by X-ray crystallography(Kanai et al. 2013b; Laursen et al. 2015; Laursen et al. 2013; Morth et al. 2011; Morth et al. 2007; Nyblom et al. 2013a; Ogawa et al. 2015; Ogawa et al. 2009; Shinoda et al. 2009; Yatime et al. 2011) and also partially several N-domain structures by X-ray crystallography (Håkansson 2003) and NMR(Mark Hilge 2003). In addition, several crystallographic structures of Ca^{2+}-ATPase were reported (Akin et al. 2013; Bublitz et al. 2015; Clausen et al. 2013; Drachmann et al. 2014; Jensen et al. 2006; Laursen et al. 2009; MacLennan & Green 2000; Moncoq et al. 2007; Obara et al. 2005; Olesen et al. 2007; Olesen et al. 2004; Paulsen et al. 2013; Sacchetto et al. 2012; Sohoel et al. 2006; Sonntag et al. 2011; Sorensen et al. 2004; Takahashi et al. 2007; Toyoshima 2008; Toyoshima et al. 2013; Toyoshima & Mizutani 2004; Toyoshima et al. 2000; Toyoshima & Nomura 2002; Winther et al. 2010; Winther et al. 2013).

The Na^+/K^+-ATPase consists of three subunits, the catalytic α-subunit with a molecular mass of about 110kDa, the β-subunit, a glycoprotein with the molecular mass of 40–60kDa (neglecting the oligosaccharides) and eventually the associated γ-subunit with the molecular mass of 8–14kDa (Collins & Leszyk 1987; Forbush III et al. 1978). The α-subunit carries out all ion transport and catalytic functions. The ion transport of Na^+ and K^+ catalyzed by Na^+/K^+-ATPase in this subunit is believed to occur via transition between two major conformational states, the

E_1Na^+ and the E_2K^+-conformations(Kaplan 2002). The α-subunit contains in a large cytoplasmic loop between the M_4 and M_5 transmembrane helices the catalytic center binding and hydrolyzing ATP. This large loop protruding far to cytoplasm comprises quite rigid subdomains and self-supporting substructures (Amler et al. 1992). Structurally it consists of two main parts, the rigid nucleotide binding domain (N-domain)(Kanai et al. 2013b; Nyblom et al. 2013a) roughly between the amino acid residues Arg^{380}–Arg^{583}, and the domain forming the Asp^{369}-phosphointermediate during ATP hydrolysis (P-domain).

The secondary structure of N-domain shows a seven-stranded antiparallel β-sheet with two helix bundles sandwiching it. In this domain Phe^{548}, Glu^{505}, Lys^{501}, Gln^{482}, Lys^{480}, Ser^{477}, Phe^{475} and Glu^{446} participate in docking of the Mg^{2+}ATP complex into its binding pocket(Kubala et al. 2003).

The P-domain consists of two parts (subdomains). Its N-terminal subdomain ranges from Lys^{347} to the residue of phosphorylation Asp^{369}. It is connected to the fourth transmembrane segment M_4 of the α-subunit. A highly negatively charged surface was found around the phosphorylation site accessible by the solvent (Tejral et al. 2007; Tejral et al. 2009). The C-terminal subdomain formed by Ala^{590}–Phe^{747} is connected to the fifth transmembrane segment M_5. These two parts (subdomains) form a typical Rossmann fold. The secondary structure of this domain can be divided into a seven-stranded parallel β-sheet with eight short associated helices (Morth et al. 2007; Ogawa et al. 2009; Shinoda et al. 2009).

Despite the relatively large amount of information available on the 3-D structure of Na^+/K^+-ATPase, the molecular mechanism of the transphosphorylation process of the terminal γ-phosphate group of ATP residing in the N-domain to the Asp^{369}-acceptor group at the P-domain is still a puzzle. Evidently, the N-domain must bend to the P-domain via a mobile hinge

84 structure. It is not clear, however, how this process is achieved on a molecular level. Hence, we
85 tried to get information on this question using molecular modeling.

Methods

Comparative modeling of the open conformation

As the solved crystal structures of Na^+/K^+-ATPase are of a non-human origin (Håkansson 2003; Kanai et al. 2013b; Laursen et al. 2015; Laursen et al. 2013; Mark Hilge 2003; Morth et al. 2011; Morth et al. 2007; Nyblom et al. 2013a; Ogawa et al. 2015; Ogawa et al. 2009; Shinoda et al. 2009; Yatime et al. 2011) only, we decided to employ the procedure of homology modeling to get its human α_2-subunit 3-D-structure. The primary amino acid sequence of the human Na^+/K^+-ATPase was retrieved from the ExPASy server (UniProt KB/TrEMBL http://www.expasy.ch/). The resulting P50993 (AT1A2_HUMAN) target human sequence in the length of 1020 amino acids for the Na^+/K^+-ATPase α_2-subunit precursor of sodium/potassium-transporting ATPase α_2-subunit, Homo sapiens, EC 3.6.3.9, was chosen (Shull et al. 1989). Five amino acids at the N-terminal beginning of this sequence compared to the translated RNA sequence do not occur in the native form (Hara et al. 1987; Kawakami et al. 1985; Ovchinnikov et al. 1986; Shull et al. 1985). Hence, they were not included in our further numbering. For modeling, known structures of Na^+/K^+-ATPase deposited at the RCSB Protein Data Bank (http://www.pdb.org/) were used. In order to create the model based on the above mentioned sequence, the solved crystal structures of Na^+/K^+-ATPase with RCSB Protein Data Bank (http://www.pdb.org/) accession codes 3B8E (Morth et al. 2007) and 3KDP(Morth et al. 2007) were used as the templates for our modeling. The multialignment of the chosen target (P50993, AT1A2_HUMAN) sequence and the two templates (3B8E, 3KDP) for open conformation was prepared by MODELLER program (salign module) (Eswar et al. 2006; Marti-Renom et al. 2000; Šali 1995; Šali & Blundell 1993). The choice of templates (solved crystal structures) was based on the species proximity (pig over shark) and absence of any cardioglycosides in the solved crystal structure, in order to get as close

to the native form as possible. Using this multialignment and the solved 3D crystal structures, we have generated thousand M_4M_5-loop models by the MODELLER (automodel module)(Eswar et al. 2006; Marti-Renom et al. 2000; Šali 1995; Šali & Blundell 1993) program. From those created models the best thirty were selected using the PROCHECK (Laskowski et al. 1993; Morris et al. 1992) and Verifi3D (Bowie et al. 1991; Lüthy et al. 1992) programs (Table I).

Comparative modeling of the closed conformation

As in the previous comparative modeling procedure, we have used the sequence P50993 (AT1A2_HUMAN) for modeling of Na^+/K^+-ATPase in the closed conformation. However, the solved crystal structures of the RCSB Protein Data Bank (http://www.pdb.org/ - accession codes 3WGU, 3WGV and 4HQJ(Kanai et al. 2013a; Nyblom et al. 2013b)) were used as the templates for our modeling. Using the above-mentioned settings for the modeling program (MODELLER see previous paragraph) we obtained ten models of Na^+/K^+-ATPase in the closed conformation. From these, the best model has been chosen using the above-mentioned PROCHEK and Verifi3D programs (Table I).

Docking, using the open and closed conformations

The best thirty models corresponding to the open conformation and the best model for the closed conformation were used for docking of Mg^{2+}•ATP complex, using the Vina-Autodock program(Trott & Olson 2010). We have decided to use the whole Mg^{2+}•ATP complex, which has been derived from structures containing ATP, deposited in RCSB Protein Data Bank (http://www.pdb.org/). The sequential docking of Mg^{2+}, followed by ATP, has not been used, since the bond between Mg^{2+} and ATP phosphates is stronger than between Mg^{2+} and –COOH groups of amino acids(Alberty 1969; Dudev et al. 1999). In addition, the same procedure was used for the model of the closed conformation.

Molecular dynamics

Molecular dynamics (MD) of the M_4M_5-loop were simulated by Gromacs (Berendsen et al. 1995; Hess et al. 2008; Lindahl et al. 2001; Van Der Spoel et al. 2005; van der Spoel et al. 2010), using the OPLS-AA potential(Jorgensen et al. 1996; Jorgensen & Tirado-Rives 1988; Kaminski et al. 2001; Meagher et al. 2003; Pranata et al. 1991) with combination of water model TIP3P(Jorgensen et al. 1983). Our protein model with or without $2Mg^{2+}$•ATP were put into a rectangular box with a 1 nm thick layer of the water molecules around and periodic boundary conditions (Berendsen et al. 1995; Hess et al. 2008; Lindahl et al. 2001; Van Der Spoel et al. 2005; van der Spoel et al. 2010).

The PME method (Darden et al. 1993) with a length parameter of 1 nm was used to describe Coulomb type electrostatic interactions and the cut-off method with a length parameter of 1 nm for the calculation of van der Waals interactions. As the first step of the MD simulation, the system of protein and water was energetically optimized using the method of steepest descents, followed by a conjugate gradient minimization algorithm with maximum $2.5x10^4$ steps and maximum force smaller than 10 $kj.mol^{-1}.nm^{-1}$ as the convergence criterion (see supplement material). The Berendsen coupling method (Berendsen et al. 1984) was employed for the temperature and pressure coupling of a system to reflect the reference temperature of 310K and the pressure of 1 bar. The leap-frog integration with 10^4 steps was used for stabilization, with integration step of 1 fs, corresponding to 10 ps simulation time to reach the equilibrium of the rectangular box (see supplement material). This stabilized rectangular box was used for the main thirty simulations with $5x10^6$ steps (2 fs single step), corresponding to 10 ns for each stabilization using the same simulation parameters as for the box stabilization. These thirty trajectories were simulated with independently generated initial conditions corresponding to a

Maxwell distribution for a temperature of 310K. The translation and rotation around the center of mass of the protein were removed, avoiding thus the simulated system distortion in the simulation box. The molecular dynamics simulation of the Na^+/K^+-ATPase in semi-open conformation with docked $2Mg^{2+}$•ATP was carried out using the same parameters as described above.

Docking to the semi-open conformation

From the charts of the time evolution of distances, the typical trajectory for the molecular dynamics of the open conformation without $2Mg^{2+}$•ATP has been chosen. The model showing a distance between Asp^{369} and Phe^{475} smaller than 2.2 nm and with the best PROCHECK and Verify3D scores were taken for docking of the $2Mg^{2+}$•ATP complex.

Results

Assembly of the static 3D computational model of Na^+/K^+-ATPase

The main goal of this work was to describe the molecular mechanism of γ-phosphate transfer from the ATP in the binding site to the phosphorylation site (Asp^{369}) of Na^+/K^+-ATPase. To achieve this, first, a static three-dimensional model of Na^+/K^+-ATPase was developed based on the latest data and information. The P50993 (AT1A2_HUMAN) human target sequence of the Na^+/K^+-ATPase α_2-isoform (sodium/potassium-transporting ATPase α_2-subunit, Homo sapiens) was used for modeling and 3D model assembling. Two templates of Na^+/K^+-ATPase structures of accession codes 3B8E(Morth et al. 2007) and 3KDP(Morth et al. 2007) were retrieved from the Protein Data Bank which were proposed by UniProt server as sequence P05024 (sodium/potassium-transporting ATPase α_1-subunit, Sus scrofa) with sequences identity 86.5% of the target sequence. The alignments for open conformation of the M_4M_5-loop were prepared with identity of the 85.6% between the corresponding sequences of the human α_2-isoform and pig α_1-isoform for the M4M5-loop. The alignment and template structures were used for comparative modeling using the MODELLER program. The obtained 3D models were verified, applying the PROCHECK and Verifi3D programs (Table I). Our modeling procedure resulted in static structures of the M_4M_5-loop of human α_2 isoform of Na^+/K^+-ATPase between Thr^{338} and Ile^{760} (see Fig. 1., with docked $2Mg^{2+}$•ATP). These models show distances around 3.26 nm between Phe^{475} as part of the ATP-binding site and the α-carbon of Asp^{369}, the acceptor site for the phosphointermediate in ATP hydrolysis.

Two ATP binding sites exist in the open conformation of Na^+/K^+-ATPase

The obtained models of the open conformation of Na^+/K^+-ATPase were tested by an *in silico* ATP-docking experiment for its ability to bind Mg^{2+}•ATP. Surprisingly, we identified two

possible docking sites (Fig. 1): The first one is in closest vicinity to Phe^{475} ("the Phe^{475} location") and the second one is close to Asp^{369}, ("the Asp^{369} location"). Both binding sites showed only slightly different docking energies. While the docking energy at the Phe^{475} location was E_b = -7.6 kcal/mol, the docking energy at the Asp^{369} location was E_b = -8.6 kcal/mol. A closer insight into our model clearly indicated interactions among π-electrons between Phe^{475} and the ATP adenine ring at the Phe^{475} location, but the interaction between ATP's phosphates with bound magnesium and the negatively charged aspartate residue was responsible for the $2Mg^{2+}$•ATP binding at the Asp^{369} location.

The amino acids found in the neighborhood of docked Mg^{2+}•ATP in both binding sites were identified and found to be in agreement with already published data(Jacobsen et al. 2002; Jorgensen et al. 2003; Jorgensen et al. 2001; Jorgensen & Pedersen 2001; Kubala et al. 2003; Pedersen et al. 2000)

High ATP concentration hinders the enzyme cycle and keeps the Na^+/K^+-ATPase at the open conformation

The structure with best docking energy for both $2Mg^{2+}$•ATP docking sites was the starting point for a molecular dynamics simulation, which revealed another surprising result. The molecular dynamics simulation in the presence of $2Mg^{2+}$•ATP (we ran two simulations series, one with $2Mg^{2+}$•ATP docked in the ATP binding site and the other in the phosphorylation site) did not result in a stable close conformation needed to phorphorylate Asp^{369} during Na^+/K^+-ATP hydrolysis. Interestingly, the enzyme preferentially remained in the open conformation in both simulations as is evident from the resulting distance distribution between α-carbons of Asp^{369}

and Phe^{475} (Fig. 2A, 2B, 3A, 3B, the distance varied from 2.5 nm to 3.4 nm, with maxima 2.9 nm and 3.1 nm respectively).

However, molecular dynamics experiments in the absence of $2Mg^{2+}$•ATP (Figure 3C) in nanosecond timescale exhibited a different pattern. This conformation was characterized by shortening of the distance between α-carbons of Asp^{369} and Phe^{475} to about d ~ 2.00 nm (Figure 3C).

Additionally, we performed 30 simulations in the absence of $2Mg^{2+}$•ATP. Yet, there was no stable result: Sometimes, the molecular dynamic simulation led to the new conformation (we will call this conformation "semi-open" conformation), but sometimes the enzyme remained in the open conformation, with the ratio open/semi-open conformation being approximately 1:1.4 (Fig. 2C, 3C). Clearly, conformational transitions between the "open" and "semi-open conformations" seem to be rather a stochastic process (Fig. 2C, 3C). Consequently, we decided to call this newly identified conformation representing a distance of 2.3 nm between Phe^{475} and Asp^{369} the "semi-open" conformation of the catalytic site of Na^+/K^+-ATPase. The semi-open conformation is characterized by the formation of a hydrogen bond between Arg^{543} and Asp^{611} (see Fig. 4).

Hinge movement, ATP binding and enzyme phosphorylation

Release and re-binding of $2Mg^{2+}$•ATP complexes at two different binding sites in the open conformation may have huge consequences for the molecular mechanism of the transphosphorylation process to Asp^{369} as part of the ATP hydrolysis of Na^+/K^+-ATPase. Most importantly is the fact that the α-subunit of Na+/K-ATPase can wobble between the "open" and "semi-open conformations" in the absence of $2Mg^{2+}$•ATP.

Naturally, the obvious question arises, whether and how the $2Mg^{2+}$•ATP complex interacts with the "semi-open conformation". Therefore, $2Mg^{2+}$•ATP molecule has been docked into the "semi-open conformation" (Fig. 5), revealing only a single $2Mg^{2+}$•ATP binding site exists. This $2Mg^{2+}$•ATP binding site in the "semi-open conformation" was formed as a sandwich structure from both, "the Phe^{475} location" and "the Asp^{369} location" as they were revealed and identified at the open conformation. Both sites have approached each other due the stochastic process in the absence of $2Mg^{2+}$•ATP, probably due to the preceding hinge movement in the absence of $2Mg^{2+}$•ATP. This binding pocket for a single $2Mg^{2+}$•ATP is characterized by the most favorable and highest docking energy of E_b = -8.8 kcal/mol.

Furthermore, docking of $2Mg^{2+}$•ATP to the "semi-open conformation" results in a further substantial shortening of the distance between the Asp^{369} and Phe^{475}. Consequently, the γ-phosphate of $2Mg^{2+}$•ATP was attracted to Asp^{369} and the mutual distance between the α-carbons of Asp^{369} and Phe^{475} decreased to approximately d=1.8 nm (Fig. 2D, 3D, majority falling in the interval 1.5-2.0 nm). This shortening can be explained as a consequence of the second phase of the hinge movement: bending of the N-domain toward the P-domain, which completes "the hinge mechanism" (Fig. 6).

In order to verify our conclusions, the closed conformation of Na^+/K^+-ATPase structure was prepared by homology modeling as well using crystallography templates (Fig. 7). The docking experiment of $2Mg^{2+}$•ATP to the "closed" conformation, revealed the existence of a single ATP binding site as well (Figure 7). Moreover, the molecular dynamic experiment with the "semi-open" sub-conformation shows that it's conformation differs from that one of the "closed"

conformation with overall RMSD < 0.3 nm, which is within the experimental error of crystallographic data.

Discussion

Multiple ATP binding sites are found in the open and semi-open conformations of the cytoplasmic M_4-M_5-loop of Na^+/K^+-ATPase

The intention of this work was to learn by inspection of a large number of related and crystallized P-type ATPases and analogous computer modeling of the cytoplasmic M_4-M_5-loop of the human α_2 isoform of Na^+/K^+-ATPase, how on a molecular level the distance is shortened between the nucleotide binding site (the N-domain) and the phosphorylation site Asp^{369} at the P-domain. The distance of 3.26 nm between both sites (in the "open" state, Fig. 6) is too high to support either the $Na^+ + Mg^{2+}$ or the Mg^{2+}-dependent transphosphorylation process or the ATP-ADP exchange reaction (Fahn et al. 1966), both the partial reactions of Na^+/K^+-ATPase. Evidently, any changes by binding of Na^+ or K^+ to their respective membrane sites must be excluded, since our analysis was restricted exclusively to the molecular events at the large cytoplasmic M_4-M_5-loop: We intended to understand the bending mechanism of the N-domain towards the P-domain.

ATP binding into the semi-open conformation leads to the hinge movement and triggers enzyme phosphorylation

We identified by molecular modeling of the cytoplasmic loop structure the existence of 3 different conformational states with the ability to bind ATP (Fig. 6). In the absence of ATP and $2Mg^{2+}$•ATP the "open" and "semi-open" conformational states are freely interconverted. The open state binds ATP in the absence of Mg^{2+} to the N-domain as previously shown (References). It may bind, however, also 2Mg2+•ATP at 2 sites, the "the Phe^{475} location" and the "the Asp^{369} location" (Fig. 1). Yet, in this open conformation, no transphosphorylation of the gamma phosphate group of ATP to Asp^{369} residing on the P-domain is possible: the terminal phosphate

of ATP is much too remote from the carboxyl group of Asp^{369}. Molecular modeling clearly showed that it is rather the newly identified semi-open conformation which binds $2Mg^{2+}$•ATP to a single site in such a way that the terminal phosphate approaches the phosphate acceptor site Asp^{369} on the P-domain leads and via a further shift to the "occluded" state may achieve its phosphorylation.

On a molecular level our model describes and is in agreement with the vast majority of published structures for the ATP binding domains of P-type ATPases (Bublitz et al. 2013; Bueno-Orovio et al. 2014; Castillo et al. 2011; Castillo et al. 2015; Fuller et al. 2013; Howland 1991; Jacobsen et al. 2002; Jensen et al. 2006; Jorgensen et al. 2003; Jorgensen et al. 2001; Jorgensen & Pedersen 2001; Kanai et al. 2013b; Kaplan 2002; Laursen et al. 2015; MacLennan & Green 2000; Morth et al. 2007; Nyblom et al. 2013a; Obara et al. 2005; Ogawa et al. 2009; Olesen et al. 2007; Pedersen et al. 2000; Sacchetto et al. 2012; Shinoda et al. 2009; Toyoshima 2008; Toyoshima et al. 2013; Toyoshima & Mizutani 2004; Toyoshima et al. 2000). Importantly, Arg^{543} is located in the N domain near the interface to the P domain (Figure 1). This residue has been shown to be essential for nucleotide binding; its substitution by Gln abolishes high-affinity binding of ATP (in the absence of Mg^{2+}) and also Na^+/K^+-ATPase activity(Pedersen et al. 2000). The free energy required overcoming the electrostatic interactions between the γ-phosphate of $2Mg^{2+}$•ATP and the carboxylate groups amounts to 7.9 kcal/mol for Asp^{369}. This value supports our model exactly. In addition, the increased binding energy of $2Mg^{2+}$•ATP is connected with a conformational transition constituting the driving force for transport of K^+ across the membrane (Howland 1991). Additionally, our molecular modeling experiments showed in docking experiments a very favorable binding energy of $2Mg^{2+}$ATP at the semi-open conformation. The strong electrostatic interaction with the negative charges of Asp^{369}, Asp^{709} and Asp^{713} with

299 $2Mg^{2+}$•ATP shows that the γ-phosphate of the tightly bound ATP are important to approach the
300 surface of the P domain in Na^+/K^+-ATPase (Jorgensen et al. 2003; Jorgensen et al. 2001;
301 Jorgensen & Pedersen 2001). This certainly leads to further bridging the gap between the N- and
302 P-domains and the formation of a "closed conformation" (Fig 6C) resulting in a type of
303 "occluded $2Mg^{2+}$•ATP " preceding the formation of a phosphointermediate in the ATP-E_1 form
304 of the α subunit of Na^+/K^+-ATPase.

305 Analogously, in the crystal structure of Ca^{2+}-ATPase in the $E_1[2Ca^{2+}-]$ form(Clausen et al. 2013;
306 Toyoshima et al. 2013; Winther et al. 2013), the N domain is separated from the P domain by a
307 distance of 2.0–2.5 nm. Such a distance is also seen in our model in the "open" conformational
308 state: The P domain of the human α_2 isoform of Na^+/K^+-ATPase is separated from the N domain
309 by a distance of less than 2 nm. Additionally, Lys^{690} appears to create a salt linkage with the
310 phosphate group as has been found in previous experiments. Mg^{2+} is essential for all phosphoryl
311 transfer reactions. The experience from Mg^{2+} binding studies is that the binding affinity and the
312 coordination pattern depend strongly on the conformational state (Pedersen et al. 2000) . Our
313 model shows this as well. Importantly, fluctuation in between the "open" and "semi-open
314 conformations" is connected with binding/unbinding of $2Mg^{2+}$•ATP to the three above
315 mentioned negatively charged residues of Asp^{709}, Asp^{713} and Asp^{369} (Fig. 1B, 4B). However,
316 binding of $2Mg^{2+}$•ATP to any site of the "open conformation" cannot lead to phosphorylation.
317 The phosphorylation process can be triggered only when the "semi-open conformation" in the
318 absence of ATP is formed. Once the semi-open conformation has been created, by forming a
319 hydrogen bond between Arg^{543} and Asp^{611} (Fig. 4), the affinity for ATP peaks, facilitating thus
320 ATP binding. The distance between Phe^{475} and Asp^{369} decreased to about 1.8 nm (corresponding
321 to 1.83 in our "closed conformation" model). This average value of the experimentally reported

distances for the "closed conformation", enables the phosphorylation of Asp^{369}, and is in accordance with the measured data (Jacobsen et al. 2002; Jorgensen et al. 2001).

To the best of our knowledge, this is the first report on the existence of three conformers of the big cytoplasmic loop binding ATP. Our finding may have important consequences for understanding the molecular mechanism of the Na^+/K^+-ATPase function. Na^+ ions have been reported to increase the activity of transphosphorylation process(Kaplan 2002). It is unclear at present, where Na^+ binds to its transport site in the transmembranal part of the enzyme and how this may affect the conformational transitions of the hinge region in the closing process approaching N- and P-domains such a way that the phosporylation of Asp^{369} as an intermediate may happen. It needs to be investigated in further studies, how, at a molecular level, high ATP concentrations lead to the release of E_2-occluded K^+. Micromolar ATP concentrations are sufficient for ATP binding (in the absence of Mg^{2+}) to the N-domain in the open state (Kubala et al. 2003; Schoner et al. 1968; Tran & Farley 1999). The effect of Mg^{2+} on the binding of ATP to the isolated N-domain has never been studied. Micromolar ATP concentrations are sufficient for the $Na^+ + Mg^{2+}$-dependent formation of the Asp^{369}-phosphointermediate (Hegyvary & Post 1971; Moczydlowski & Fortes 1981). Millimolar ATP concentrations are necessary for the overall Na^+/K^+-activated ATP hydrolysis necessary for Na^+/K^+-transport. High (millimolar) ATP concentrations are necessary to result in the de-occlusion of K^+ from its transmembrane site. Might it be that the existence of 2 ATP sites in the "open conformation" of the cytoplasmic loop (Fig 1) represents a situation of opening of the closed catalytic site for MgATP at high concentrations of the energy substrate. It is well known that K^+ ions are on its way from the outside to the inside of the cell included into the transmembrane part of Na^+/K^+-ATPase. High concentrations of MgATP are necessary to release occludes K+ from the sodium pump into the

cytoplasm. One may speculate that binding of MgATP at millimolar concentrations may lead to a shift of the “closed conformation” to the “open conformation”. i.e the displacement of the N-domain via the hinge mechanism from the P-domain due to binding of millimolar MgATP to the N-domain (Fig. 8).

References

Akin BL, Hurley TD, Chen Z, and Jones LR. 2013. The structural basis for phospholamban inhibition of the calcium pump in sarcoplasmic reticulum. *J Biol Chem* 288:30181-30191. 10.1074/jbc.M113.501585

Alberty RA. 1969. Standard Gibbs Free Energy, Enthalpy, and Entropy Changes as a Function of pH and pMg for Several Reactions Involving Adenosine Phosphates. *Journal of Biological Chemistry* 244:3290-3302.

Amler E, Abbott A, and Ball WJ. 1992. Structural dynamics and oligomeric interactions of Na+,K(+)-ATPase as monitored using fluorescence energy transfer. *Biophysical Journal* 61:553-568. 10.1016/s0006-3495(92)81859-3

Berendsen HJC, Postma JPM, van Gunsteren WF, DiNola A, and Haak JR. 1984. Molecular dynamics with coupling to an external bath. *The Journal of Chemical Physics* 81:3684-3690. doi:10.1063/1.448118

Berendsen HJC, van der Spoel D, and van Drunen R. 1995. GROMACS: A message-passing parallel molecular dynamics implementation. *Computer Physics Communications* 91:43-56.

Bowie JU, Luthy R, and Eisenberg D. 1991. A method to identify protein sequences that fold into a known three-dimensional structure. *Science* 253:164-170. 10.1126/science.1853201

Bublitz M, Musgaard M, Poulsen H, Thogersen L, Olesen C, Schiott B, Morth JP, Moller JV, and Nissen P. 2013. Ion pathways in the sarcoplasmic reticulum Ca2+-ATPase. *J Biol Chem* 288:10759-10765. 10.1074/jbc.R112.436550

372 Bublitz M, Nass K, Drachmann ND, Markvardsen AJ, Gutmann MJ, Barends TRM, Mattle D,
373 Shoeman RL, Doak RB, Boutet S, Messerschmidt M, Seibert MM, Williams GJ, Foucar
374 L, Reinhard L, Sitsel O, Gregersen JL, Clausen JD, Boesen T, Gotfryd K, Wang K-T,
375 Olesen C, Møller JV, Nissen P, and Schlichting I. 2015. Structural studies of P-type
376 ATPase–ligand complexes using an X-ray free-electron laser. *IUCrJ* 2:409-420.
377 10.1107/S2052252515008969
378 Bueno-Orovio A, Sanchez C, Pueyo E, and Rodriguez B. 2014. Na/K pump regulation of cardiac
379 repolarization: insights from a systems biology approach. *Pflugers Arch* 466:183-193.
380 10.1007/s00424-013-1293-1
381 Castillo JP, De Giorgis D, Basilio D, Gadsby DC, Rosenthal JJ, Latorre R, Holmgren M, and
382 Bezanilla F. 2011. Energy landscape of the reactions governing the Na+ deeply occluded
383 state of the Na+/K+-ATPase in the giant axon of the Humboldt squid. *Proc Natl Acad Sci*
384 *U S A* 108:20556-20561. 10.1073/pnas.1116439108
385 Castillo JP, Rui H, Basilio D, Das A, Roux B, Latorre R, Bezanilla F, and Holmgren M. 2015.
386 Mechanism of potassium ion uptake by the Na(+)/K(+)-ATPase. *Nat Commun* 6:7622.
387 10.1038/ncomms8622
388 Clausen JD, Bublitz M, Arnou B, Montigny C, Jaxel C, Møller JV, Nissen P, Andersen JP, and
389 le Maire M. 2013. SERCA mutant E309Q binds two Ca^{2+} ions but adopts a catalytically
390 incompetent conformation: Structure and function of SERCA mutant E309Q. *The EMBO*
391 *Journal* 32:3231-3243. 10.1038/emboj.2013.250
392 Collins JH, and Leszyk J. 1987. ". gamma. Subunit" of sodium-potassium-ATPase, a small,
393 amphiphilic protein with a unique amino acid sequence. *Biochemistry* 26:8665-8668.

394 Darden T, York D, and Pedersen L. 1993. Particle mesh Ewald: An N·log(N) method for Ewald
395 sums in large systems. *The Journal of Chemical Physics* 98:10089-10092.
396 doi:10.1063/1.464397
397 Drachmann ND, Olesen C, Møller JV, Guo Z, Nissen P, and Bublitz M. 2014. Comparing crystal
398 structures of Ca2+-ATPase in the presence of different lipids. FEBS Journal. p 4249-
399 4262.
400 Dudev T, Cowan JA, and Lim C. 1999. Competitive Binding in Magnesium Coordination
401 Chemistry: Water versus Ligands of Biological Interest. *Journal of the American*
402 *Chemical Society* 121:7665-7673. 10.1021/ja984470t
403 Eswar N, Webb B, Marti-Renom MA, Madhusudhan MS, Eramian D, Shen MY, Pieper U, and
404 Sali A. 2006. Comparative protein structure modeling using Modeller. *Curr Protoc*
405 *Bioinformatics* Chapter 5:Unit 5 6. 10.1002/0471250953.bi0506s15
406 Fahn S, Koval GJ, and Albers RW. 1966. Sodium-Potassium-activated Adenosine
407 Triphosphatase of Electrophorus Electric Organ I. AN ASSOCIATED SODIUM-
408 ACTIVATED TRANSPHOSPHORYLATION. *Journal of Biological Chemistry*
409 241:1882-1889.
410 Forbush III B, Kaplan JH, and Hoffman JF. 1978. Characterization of a new photoaffinity
411 derivative of ouabain: labeling of the large polypeptide and of a proteolipid component of
412 the (sodium-potassium ion)-dependent ATPase. *Biochemistry* 17:3667-3676.
413 Fuller W, Tulloch LB, Shattock MJ, Calaghan SC, Howie J, and Wypijewski KJ. 2013.
414 Regulation of the cardiac sodium pump. *Cell Mol Life Sci* 70:1357-1380.
415 10.1007/s00018-012-1134-y

416 Håkansson KO. 2003. The Crystallographic Structure of Na,K-ATPase N-domain at 2.6Å
417 Resolution. *Journal of Molecular Biology* 332:1175-1182. 10.1016/j.jmb.2003.07.012
418 Hara Y, Urayama O, Kawakami K, Nojima H, Nagamune H, Kojima T, Ohta T, Nagano K, and
419 Nakao M. 1987. Primary Structures of Two Types of Alpha-Subunit of Rat Brain Na+,
420 K+-ATPase Deduced from cDNA Sequences. *The Journal of Biochemistry* 102:43-58.
421 Hegyvary C, and Post RL. 1971. Binding of adenosine triphosphate to sodium and potassium
422 ion-stimulated adenosine triphosphatase. *J Biol Chem* 246:5234-5240.
423 Hess B, Kutzner C, van der Spoel D, and Lindahl E. 2008. GROMACS 4: Algorithms for Highly
424 Efficient, Load-Balanced, and Scalable Molecular Simulation. *Journal of Chemical*
425 *Theory and Computation* 4:435-447. 10.1021/ct700301q
426 Howland JL. 1991. Electrogenic ion pumps by Peter Läuger. *Biochemical Education* 20:243.
427 10.1016/0307-4412(92)90213-6
428 Jacobsen MD, Pedersen PA, and Jorgensen PL. 2002. Importance of Na,K-ATPase residue alpha
429 1-Arg544 in the segment Arg544-Asp567 for high-affinity binding of ATP, ADP, or
430 MgATP. *Biochemistry* 41:1451-1456.
431 Jensen A-ML, Sørensen TL-M, Olesen C, Møller JV, and Nissen P. 2006. Modulatory and
432 catalytic modes of ATP binding by the calcium pump. *The EMBO Journal* 25:2305-2314.
433 10.1038/sj.emboj.7601135
434 Jorgensen PL, Hakansson KO, and Karlish SJ. 2003. Structure and mechanism of Na,K-ATPase:
435 functional sites and their interactions. *Annu Rev Physiol* 65:817-849.
436 10.1146/annurev.physiol.65.092101.142558

437 Jorgensen PL, Jorgensen JR, and Pedersen PA. 2001. Role of conserved TGDGVND-loop in
438 Mg2+ binding, phosphorylation, and energy transfer in Na,K-ATPase. *J Bioenerg*
439 *Biomembr* 33:367-377.
440 Jorgensen PL, and Pedersen PA. 2001. Structure–function relationships of Na+, K+, ATP, or
441 Mg2+ binding and energy transduction in Na,K-ATPase. *Biochimica et Biophysica Acta*
442 *(BBA) - Bioenergetics* 1505:57-74. 10.1016/s0005-2728(00)00277-2
443 Jorgensen WL, Chandrasekhar J, Madura JD, Impey RW, and Klein ML. 1983. Comparison of
444 simple potential functions for simulating liquid water. *The Journal of Chemical Physics*
445 79:926-935. doi:10.1063/1.445869
446 Jorgensen WL, Maxwell DS, and Tirado-Rives J. 1996. Development and Testing of the OPLS
447 All-Atom Force Field on Conformational Energetics and Properties of Organic Liquids.
448 *Journal of the American Chemical Society* 118:11225-11236. 10.1021/ja9621760
449 Jorgensen WL, and Tirado-Rives J. 1988. The OPLS [optimized potentials for liquid
450 simulations] potential functions for proteins, energy minimizations for crystals of cyclic
451 peptides and crambin. *Journal of the American Chemical Society* 110:1657-1666.
452 10.1021/ja00214a001
453 Kaminski GA, Friesner RA, Tirado-Rives J, and Jorgensen WL. 2001. Evaluation and
454 Reparametrization of the OPLS-AA Force Field for Proteins via Comparison with
455 Accurate Quantum Chemical Calculations on Peptides†. *The Journal of Physical*
456 *Chemistry B* 105:6474-6487. 10.1021/jp003919d
457 Kanai R, Ogawa H, Vilsen B, Cornelius F, and Toyoshima C. 2013a. Crystal structure of a Na+-
458 bound Na+,K+-ATPase preceding the E1P state. *Nature* 502:201-206.
459 10.1038/nature12578

460 Kanai R, Ogawa H, Vilsen B, Cornelius F, and Toyoshima C. 2013b. Crystal structure of a Na+-
461 bound Na+,K+-ATPase preceding the E1P state. *Nature* 502:201-206.
462 10.1038/nature12578
463 Kaplan JH. 2002. Biochemistry of Na,K-ATPase. *Annu Rev Biochem* 71:511-535.
464 10.1146/annurev.biochem.71.102201.141218
465 Kawakami K, Noguchi S, Noda M, Takahashi H, Ohta T, Kawamura M, Nojima H, Nagano K,
466 Hirose T, Inayama S, Hayashida H, Miyata T, and Numa S. 1985. Primary structure of
467 the α-subunit of Torpedo californica (Na+ + K+)ATPase deduced from cDNA sequence.
468 *Nature* 316:733-736. 10.1038/316733a0
469 Kubala M, Teisinger J, Ettrich R, Hofbauerova K, Kopecky V, Jr., Baumruk V, Krumscheid R,
470 Plasek J, Schoner W, and Amler E. 2003. Eight amino acids form the ATP recognition
471 site of Na(+)/K(+)-ATPase. *Biochemistry* 42:6446-6452. 10.1021/bi034162u
472 Laskowski RA, MacArthur MW, Moss DS, and Thornton JM. 1993. PROCHECK: a program to
473 check the stereochemical quality of protein structures. *Journal of Applied*
474 *Crystallography* 26:283-291.
475 Laursen M, Bublitz M, Moncoq K, Olesen C, Møller JV, Young HS, Nissen P, and Morth JP.
476 2009. Cyclopiazonic Acid Is Complexed to a Divalent Metal Ion When Bound to the
477 Sarcoplasmic Reticulum Ca2+-ATPase. *Journal of Biological Chemistry* 284:13513-
478 13518. 10.1074/jbc.C900031200
479 Laursen M, Gregersen JL, Yatime L, Nissen P, and Fedosova NU. 2015. Structures and
480 characterization of digoxin- and bufalin-bound Na+,K+-ATPase compared with the
481 ouabain-bound complex. *Proc Natl Acad Sci U S A* 112:1755-1760.
482 10.1073/pnas.1422997112

483 Laursen M, Yatime L, Nissen P, and Fedosova NU. 2013. Crystal structure of the high-affinity
484 Na+K+-ATPase-ouabain complex with Mg2+ bound in the cation binding site. *Proc Natl*
485 *Acad Sci U S A* 110:10958-10963. 10.1073/pnas.1222308110
486 Lindahl E, Hess B, and van der Spoel D. 2001. GROMACS 3.0: a package for molecular
487 simulation and trajectory analysis. *Journal of Molecular Modeling* 7:306-317.
488 Lüthy R, Bowie JU, and Eisenberg D. 1992. Assessment of protein models with three-
489 dimensional profiles. *Published online: 05 March 1992* 356:83-85. 10.1038/356083a0
490 MacLennan DH, and Green NM. 2000. Structural biology: Pumping ions. *Nature* 405:633-634.
491 10.1038/35015206
492 Mark Hilge GS, Geerten W Vuister, Peter Güntert, Sergio M Gloor, Jan Pieter Abrahams. 2003.
493 ATP-induced conformational changes of the nucleotide-binding domain of Na,K-
494 ATPase. *Nature Structural Biology* 10:468-474.
495 Marti-Renom MA, Stuart AC, Fiser A, Sanchez R, Melo F, and Sali A. 2000. Comparative
496 protein structure modeling of genes and genomes. *Annu Rev Biophys Biomol Struct*
497 29:291-325. 10.1146/annurev.biophys.29.1.291
498 Meagher KL, Redman LT, and Carlson HA. 2003. Development of polyphosphate parameters
499 for use with the AMBER force field. *Journal of Computational Chemistry* 24:1016–1025.
500 10.1002/jcc.10262
501 Moczydlowski EG, and Fortes PA. 1981. Inhibition of sodium and potassium adenosine
502 triphosphatase by 2',3'-O-(2,4,6-trinitrocyclohexadienylidene) adenine nucleotides.
503 Implications for the structure and mechanism of the Na:K pump. *J Biol Chem* 256:2357-
504 2366.

505 Moncoq K, Trieber CA, and Young HS. 2007. The Molecular Basis for Cyclopiazonic Acid
506 Inhibition of the Sarcoplasmic Reticulum Calcium Pump. *Journal of Biological*
507 *Chemistry* 282:9748-9757. 10.1074/jbc.M611653200
508 Morris AL, MacArthur MW, Hutchinson EG, and Thornton JM. 1992. Stereochemical quality of
509 protein structure coordinates. *Proteins: Structure, Function, and Bioinformatics* 12:345–
510 364. 10.1002/prot.340120407
511 Morth JP, Pedersen BP, Buch-Pedersen MJ, Andersen JP, Vilsen B, Palmgren MG, and Nissen
512 P. 2011. A structural overview of the plasma membrane Na+,K+-ATPase and H+-
513 ATPase ion pumps. *Nat Rev Mol Cell Biol* 12:60-70. 10.1038/nrm3031
514 Morth JP, Pedersen BP, Toustrup-Jensen MS, Sorensen TL, Petersen J, Andersen JP, Vilsen B,
515 and Nissen P. 2007. Crystal structure of the sodium-potassium pump. *Nature* 450:1043-
516 1049. 10.1038/nature06419
517 Nyblom M, Poulsen H, Gourdon P, Reinhard L, Andersson M, Lindahl E, Fedosova N, and
518 Nissen P. 2013a. Crystal structure of Na+, K(+)-ATPase in the Na(+)-bound state.
519 *Science* 342:123-127. 10.1126/science.1243352
520 Nyblom M, Poulsen H, Gourdon P, Reinhard L, Andersson M, Lindahl E, Fedosova N, and
521 Nissen P. 2013b. Crystal Structure of Na+, K+-ATPase in the Na+-Bound State. *Science*
522 342:123-127. 10.1126/science.1243352
523 Obara K, Miyashita N, Xu C, Toyoshima I, Sugita Y, Inesi G, and Toyoshima C. 2005.
524 Structural role of countertransport revealed in Ca2+ pump crystal structure in the absence
525 of Ca2+. *Proc Natl Acad Sci U S A* 102:14489-14496. 10.1073/pnas.0506222102

526 Ogawa H, Cornelius F, Hirata A, and Toyoshima C. 2015. Sequential substitution of K(+) bound
527 to Na(+),K(+)-ATPase visualized by X-ray crystallography. *Nat Commun* 6:8004.
528 10.1038/ncomms9004
529 Ogawa H, Shinoda T, Cornelius F, and Toyoshima C. 2009. Crystal structure of the sodium-
530 potassium pump (Na+,K+-ATPase) with bound potassium and ouabain. *Proc Natl Acad*
531 *Sci U S A* 106:13742-13747. 10.1073/pnas.0907054106
532 Olesen C, Picard M, Winther A-ML, Gyrup C, Morth JP, Oxvig C, Møller JV, and Nissen P.
533 2007. The structural basis of calcium transport by the calcium pump. *Nature* 450:1036-
534 1042. 10.1038/nature06418
535 Olesen C, Sørensen TL-M, Nielsen RC, Møller JV, and Nissen P. 2004. Dephosphorylation of
536 the Calcium Pump Coupled to Counterion Occlusion. *Science* 306:2251-2255.
537 10.1126/science.1106289
538 Ovchinnikov YA, Modyanov NN, Broude NE, Petrukhin KE, Grishin AV, Arzamazova NM,
539 Aldanova NA, Monastyrskaya GS, and Sverdlov ED. 1986. Pig kidney Na+,K+-ATPase:
540 Primary structure and spatial organization. *FEBS Lett* 201:237-245. 16/0014-
541 5793(86)80616-0
542 Paulsen ES, Villadsen J, Tenori E, Liu H, Bonde DF, Lie MA, Bublitz M, Olesen C, Autzen HE,
543 Dach I, Sehgal P, Nissen P, Møller JV, Schiøtt B, and Christensen SB. 2013. Water-
544 Mediated Interactions Influence the Binding of Thapsigargin to Sarco/Endoplasmic
545 Reticulum Calcium Adenosinetriphosphatase. *Journal of Medicinal Chemistry* 56:3609-
546 3619. 10.1021/jm4001083

547 Pedersen PA, Jorgensen JR, and Jorgensen PL. 2000. Importance of conserved alpha -subunit
548 segment 709GDGVND for Mg2+ binding, phosphorylation, and energy transduction in
549 Na,K-ATPase. *J Biol Chem* 275:37588-37595. 10.1074/jbc.M005610200
550 Pranata J, Wierschke SG, and Jorgensen WL. 1991. OPLS potential functions for nucleotide
551 bases. Relative association constants of hydrogen-bonded base pairs in chloroform.
552 *Journal of the American Chemical Society* 113:2810-2819. 10.1021/ja00008a002
553 Sacchetto R, Bertipaglia I, Giannetti S, Cendron L, Mascarello F, Damiani E, Carafoli E, and
554 Zanotti G. 2012. Crystal structure of sarcoplasmic reticulum Ca2+-ATPase (SERCA)
555 from bovine muscle. *Journal of Structural Biology* 178:38-44. 10.1016/j.jsb.2012.02.008
556 Shinoda T, Ogawa H, Cornelius F, and Toyoshima C. 2009. Crystal structure of the sodium-
557 potassium pump at 2.4 A resolution. *Nature* 459:446-450. 10.1038/nature07939
558 Shull GE, Schwartz A, and Lingrel JB. 1985. Amino-acid sequence of the catalytic subunit of the
559 (Na+ + K+)ATPase deduced from a complementary DNA. *Nature* 316:691-695.
560 10.1038/316691a0
561 Shull MM, Pugh DG, and Lingrel JB. 1989. Characterization of the human Na,K-ATPase alpha
562 2 gene and identification of intragenic restriction fragment length polymorphisms.
563 *Journal of Biological Chemistry* 264:17532-17543.
564 Schoner W, Beusch R, and Kramer R. 1968. On the mechanism of Na plus and K plus-stimulated
565 hydrolysis of adenosine triphosphate. 2. Comparison of nucleotide specificities of Na
566 plus and K plus-activated ATPase and Na plus-dependent phosphorylation of cell
567 membranes. *Eur J Biochem* 7:102-110.
568 Sohoel H, Jensen AM, Moller JV, Nissen P, Denmeade SR, Isaacs JT, Olsen CE, and
569 Christensen SB. 2006. Natural products as starting materials for development of second-

generation SERCA inhibitors targeted towards prostate cancer cells. *Bioorg Med Chem* 14:2810-2815. 10.1016/j.bmc.2005.12.001

Sonntag Y, Musgaard M, Olesen C, Schiøtt B, Møller JV, Nissen P, and Thøgersen L. 2011. Mutual adaptation of a membrane protein and its lipid bilayer during conformational changes. *Nat Commun* 2:304. 10.1038/ncomms1307

Sorensen TL, Moller JV, and Nissen P. 2004. Phosphoryl transfer and calcium ion occlusion in the calcium pump. *Science* 304:1672-1675. 10.1126/science.1099366

Šali A. 1995. Comparative protein modeling by satisfaction of spatial restraints. *Mol Med Today* 1:270-277. 10.1016/S1357-4310(95)91170-7

Šali A, and Blundell TL. 1993. Comparative Protein Modelling by Satisfaction of Spatial Restraints. *Journal of Molecular Biology* 234:779-815. 10.1006/jmbi.1993.1626

Takahashi M, Kondou Y, and Toyoshima C. 2007. Interdomain communication in calcium pump as revealed in the crystal structures with transmembrane inhibitors. *Proceedings of the National Academy of Sciences* 104:5800-5805. 10.1073/pnas.0700979104

Tejral G, Kolácná L, Kotyk A, and Amler E. 2007. Comparative modeling of the H_4-H_5-loop of the α_2-isoform of Na^+/K^+-ATPase α-subunit in the E_1 conformation. *Physiological Research / Academia Scientiarum Bohemoslovaca* 56 Suppl 1:S143-151.

Tejral G, Kolácná L, Schoner W, and Amler E. 2009. The π-helix formation between Asp^{369} and Thr^{375} as a key factor in E_1-E_2 conformational change of Na+/K+-ATPase. *Physiological Research / Academia Scientiarum Bohemoslovaca* 58:583-589.

Toyoshima C. 2008. Structural aspects of ion pumping by Ca2+-ATPase of sarcoplasmic reticulum. *Arch Biochem Biophys* 476:3-11. 10.1016/j.abb.2008.04.017

592 Toyoshima C, Iwasawa S, Ogawa H, Hirata A, Tsueda J, and Inesi G. 2013. Crystal structures of
593 the calcium pump and sarcolipin in the Mg2+-bound E1 state. *Nature* 495:260-264.
594 10.1038/nature11899
595 Toyoshima C, and Mizutani T. 2004. Crystal structure of the calcium pump with a bound ATP
596 analogue. *Nature* 430:529-535. 10.1038/nature02680
597 Toyoshima C, Nakasako M, Nomura H, and Ogawa H. 2000. Crystal structure of the calcium
598 pump of sarcoplasmic reticulum at 2.6 Å resolution. *Nature* 405:647-655.
599 10.1038/35015017
600 Toyoshima C, and Nomura H. 2002. Structural changes in the calcium pump accompanying the
601 dissociation of calcium. *Nature* 418:605-611. 10.1038/nature00944
602 Tran CM, and Farley RA. 1999. Catalytic activity of an isolated domain of Na,K-ATPase
603 expressed in Escherichia coli. *Biophys J* 77:258-266. 10.1016/S0006-3495(99)76887-6
604 Trott O, and Olson AJ. 2010. AutoDock Vina: improving the speed and accuracy of docking
605 with a new scoring function, efficient optimization, and multithreading. *J Comput Chem*
606 31:455-461. 10.1002/jcc.21334
607 Van Der Spoel D, Lindahl E, Hess B, Groenhof G, Mark AE, and Berendsen HJC. 2005.
608 GROMACS: Fast, flexible, and free. *J Comput Chem* 26:1701–1718. 10.1002/jcc.20291
609 van der Spoel D, Lindahl E, Hess B, van Buuren AR, Apol E, Meulenhoff PJ, Tieleman DP,
610 Sijbers ALTM, Feenstra KA, van Drunen R, and Berendsen HJC. 2010. *Gromacs User*
611 *Manual version 4.5*.
612 Winther A-ML, Liu H, Sonntag Y, Olesen C, Maire Ml, Soehoel H, Olsen C-E, Christensen SB,
613 Nissen P, and Møller JV. 2010. Critical Roles of Hydrophobicity and Orientation of Side
614 Chains for Inactivation of Sarcoplasmic Reticulum Ca2+-ATPase with Thapsigargin and

615 Thapsigargin Analogs. *Journal of Biological Chemistry* 285:28883-28892.
616 10.1074/jbc.M110.136242
617 Winther AM, Bublitz M, Karlsen JL, Moller JV, Hansen JB, Nissen P, and Buch-Pedersen MJ.
618 2013. The sarcolipin-bound calcium pump stabilizes calcium sites exposed to the
619 cytoplasm. *Nature* 495:265-269. 10.1038/nature11900
620 Yatime L, Laursen M, Morth JP, Esmann M, Nissen P, and Fedosova NU. 2011. Structural
621 insights into the high affinity binding of cardiotonic steroids to the Na+,K+-ATPase. *J*
622 *Struct Biol* 174:296-306. 10.1016/j.jsb.2010.12.004

623

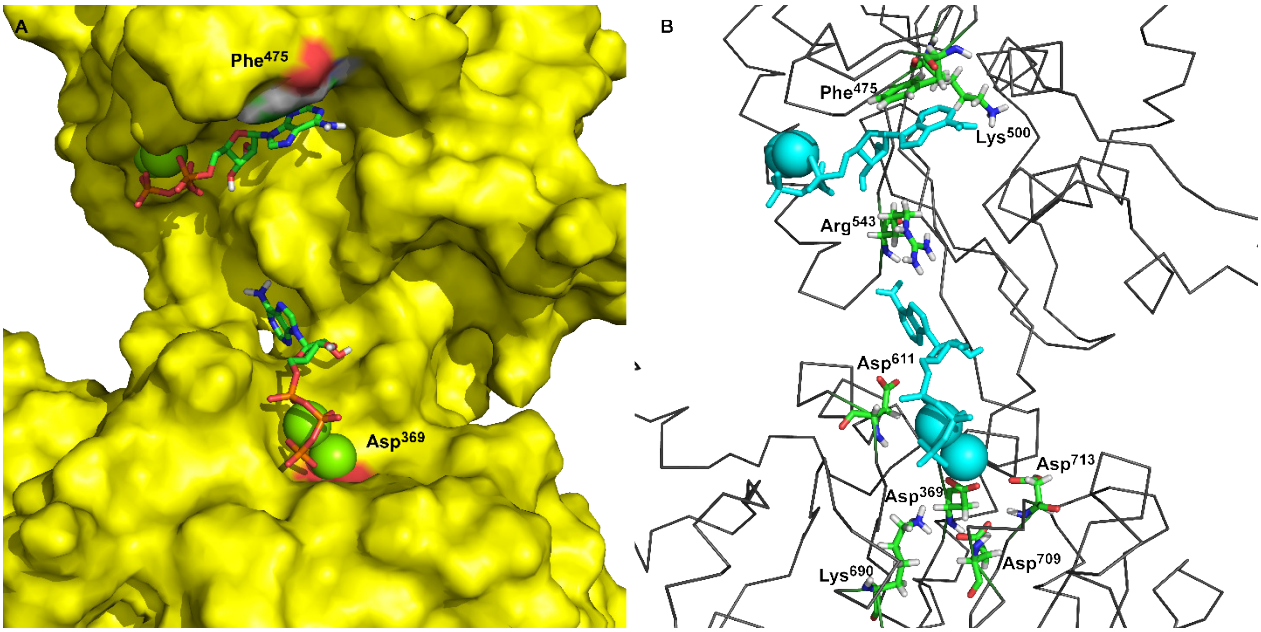

Figure 1. Two ATP binding sites in "open" conformation.

A) ATP bound near Phe^{475} has docking energy -7.6 kcal/mol, ATP near Asp^{369} has docking energy -8.9 kcal/mol.

B) The interacting amino acids with docked $2Mg^{2+}ATP$ – both binding sites

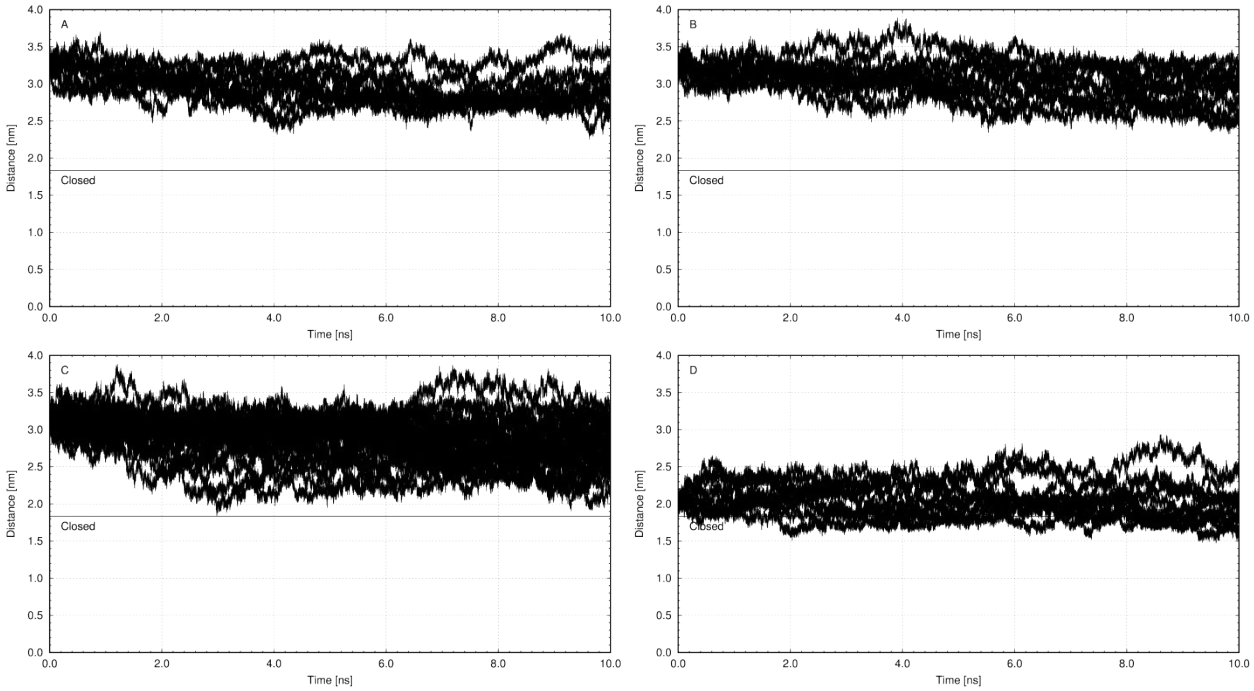

631

632 **Figure 2**.

633 A) Molecular dynamics simulation of the model in open state (change of distance between Phe^{475}

634 and Asp^{369} during simulation) with $2Mg^{2+}ATP$ interacting with Phe^{475}.

635 B) Molecular dynamics simulation of the model in open state (change of distance between Phe^{475}

636 and Asp^{369} during simulation) $2Mg^{2+}ATP$ interacting with Asp^{369}.

637 C) Molecular dynamics simulation of the model in open state (change of distance between Phe^{475}

638 and Asp^{369} during simulation) without $2Mg^{2+}ATP$

639 D) Molecular dynamics simulation of the model in open state (change of distance between Phe^{475}

640 and Asp^{369} during simulation) with $2Mg^{2+}ATP$ docked in semi-open conformation (C), and

641 interacting with both Phe^{475} and Asp^{369} (closed conformation).

642

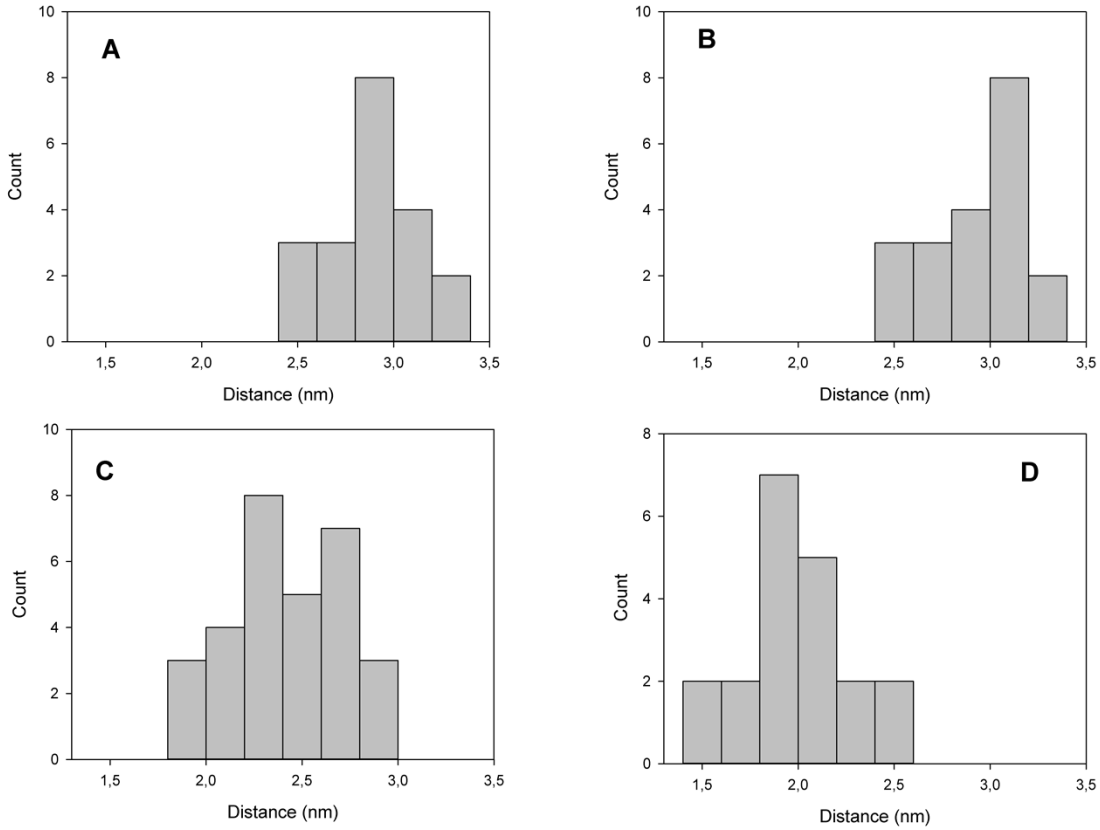

643

644 **Figure 3**.

645 A) Resulting distance distribution between Phe^{475} and Asp^{369} at the end of simulation with

646 $2Mg^{2+}ATP$ interacting with Phe^{475}.

647 B) Resulting distance distribution between Phe^{475} and Asp^{369} at the end of simulation with

648 $2Mg^{2+}ATP$ interacting with Asp^{369}.

649 C) Resulting distance distribution between Phe^{475} and Asp^{369} at the end of simulation without

650 $2Mg^{2+}ATP$

651 D) Resulting distance distribution between Phe^{475} and Asp^{369} at the end of simulation with
652 2Mg^{2+}ATP docked in semi-open conformation (C), and interacting with both Phe^{475} and Asp^{369}
653 (closed conformation).

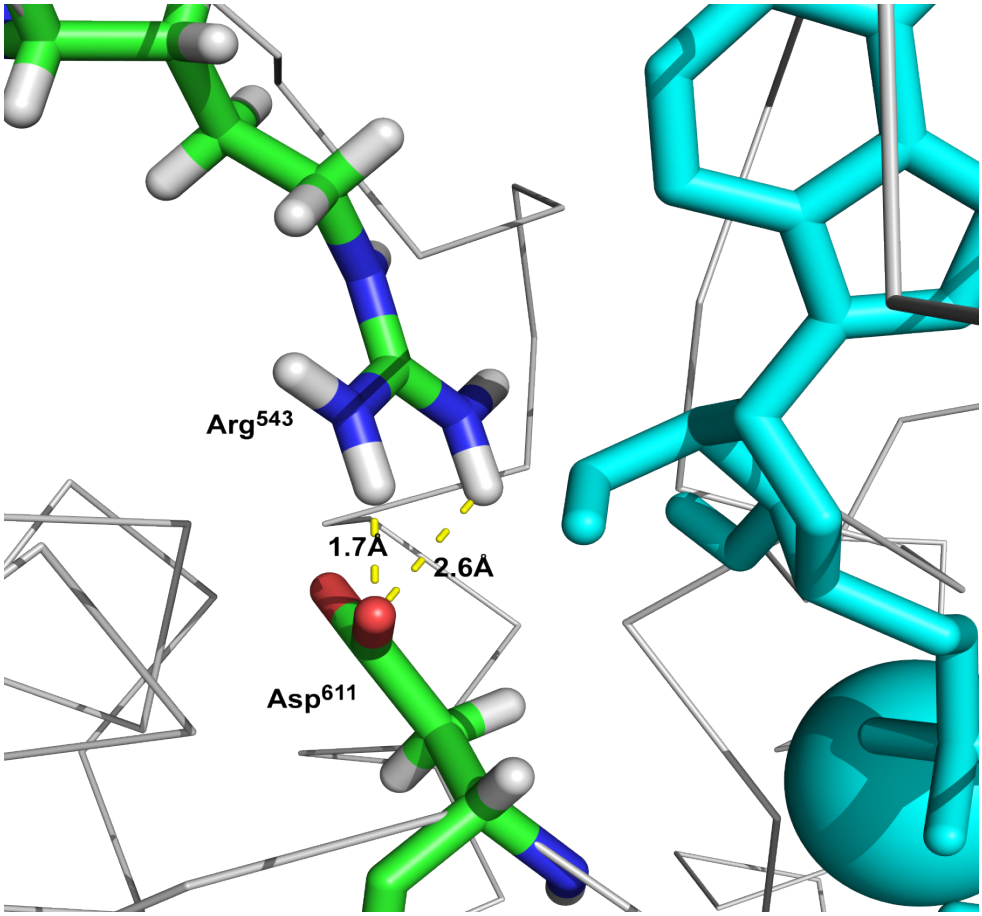

654
655
656 **Figure 4**. The hydrogen bonds between Arg^{543} and Asp^{611} formed in semi-open state.
657

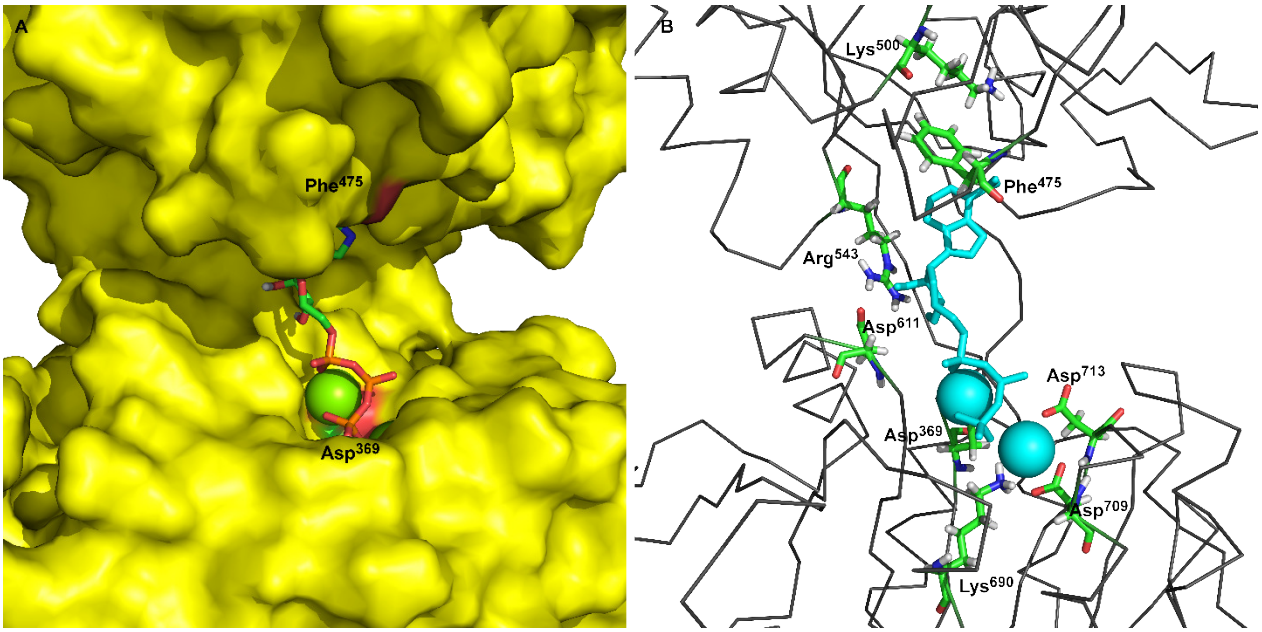

658

659 **Figure 5** Docking of $2Mg^{2+}$•ATP to the "semi-open" conformation. The simultaneous

660 interaction of $2Mg^{2+}$•ATP with Phe^{475} and Asp^{369} can be identified.

661

662

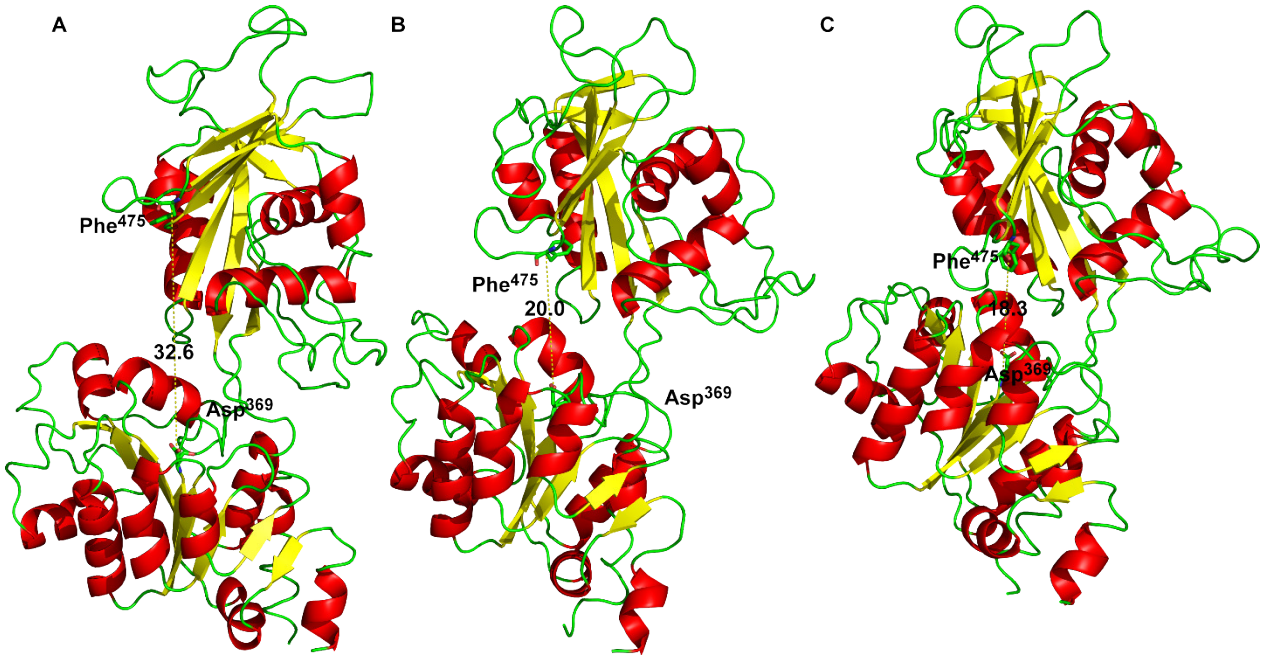

663

664 **Figure 6** The three conformational states of Na^+/K^+-ATPase (distances are in Å). From the left:

665 A) Open conformation, B) "Semi-open" conformation and C) Closed conformation.

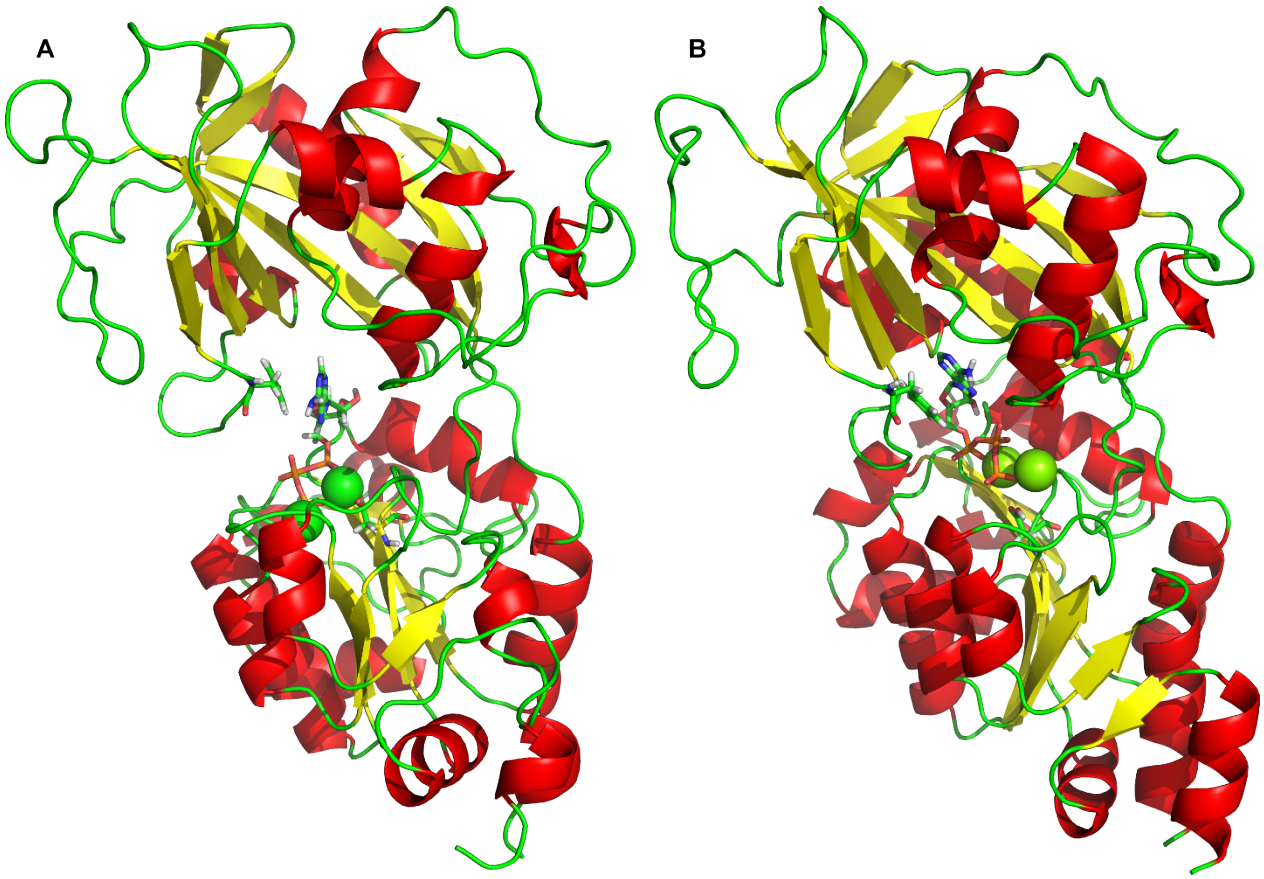

Figure 7

A) The conformation received as the result of the molecular dynamic experiment with docked $2Mg^{2+}$•ATP (closed state).

B) The conformation received as the result of the homology modeling of Na^+/K^+-ATPase in the "closed" state, with docked $2Mg^{2+}$ATP. The overall difference between these two conformations has RMSD=0.27 nm, which is within the error of the crystallographic data.

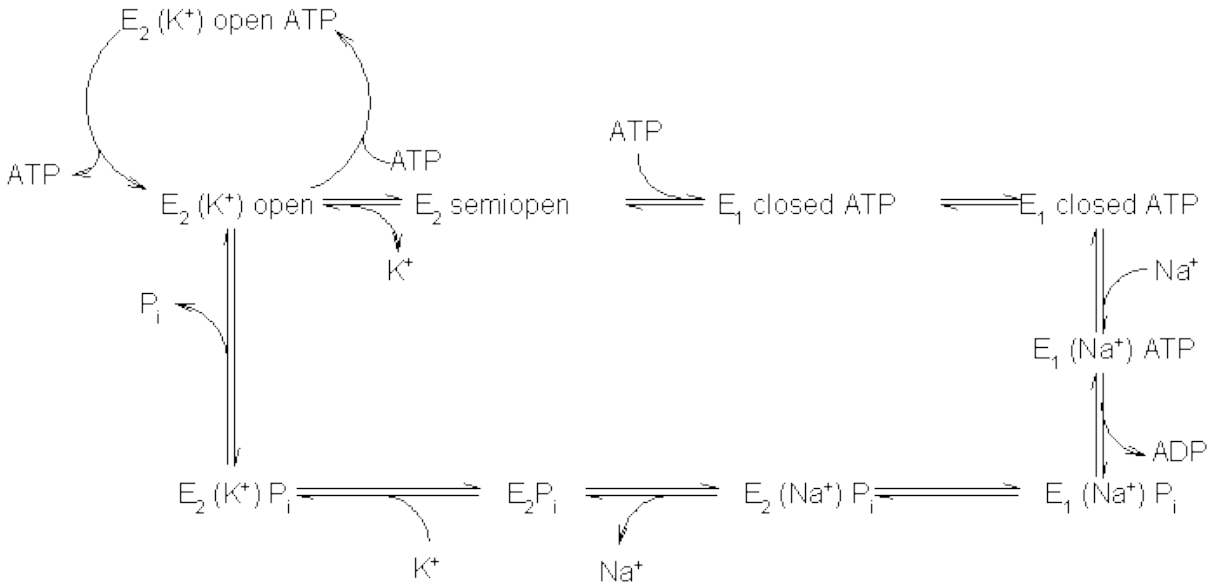

676

677 **Figure 8** Reaction scheme of Na^+/K^+-ATPase explaining the possible functions of the "open",

678 "semi-open" and "closed" conformations of the big cytoplasmic loop within the export of Na^+

679 and import of K^+ by the sodium pump.

680

681

Model	Compound (pdb code)	Ramachandran plot: Percent of aminoacids in allowed regions	Procheck: Overall G-factor	Verify3D: percent of residues that had an averaged 3D-1D score >= 0.2	Total Energy (kJ/mol) (GROMOS96)
Open conformation	3b8eA (crystal structure)	93.6	0.01	88.44	-4645.14
	3b8eC (crystal structure)	93.3	0.01	91.98	-4644.72
	3kdpA (crystal structure)	95.8	-0.31	92.69	-3484.95
	3kdpC (crystal structure)	96.3	-0.32	92.69	-2921.80
	Model of open conformation	98.2	-0.21	97.64	-14113.98
Closed conformation	3wguA (crystal structure)	98.9	-0.07	99.53	-10732.51
	3wguC (crystal structure)	99.8	0.01	97.17	-13461.95
	3wgvA (crystal structure)	98.7	-0.10	96.70	-10132.11
	3wgvC (crystal structure)	100.0	-0.02	95.99	-12870.88
	4hqjA (crystal structure)	99.2	0.10	98.58	-12983.13
	4hqjC (crystal structure)	99.4	0.13	98.58	-13081.49
	Model of closed conformation	99.5	0.06	96.93	-7995.71

682

683 **Table I** The assessment of homology model quality (compared to the ones of template crystal
684 structures).